Do Trees Need Umbrellas? Using Raytracing to Assess the Heat Stress of Trees in Cities

Yuhao Lu[1], Justin McCarty[2], Michael Fitzpatrick[3], Xun Liu[4], Dale Wiebe[3]

[1]Faculty of Architecture, University of Manitoba, Winnipeg/Canada · yuhao.lu@umanitoba.ca
[2]Chair of Architecture and Building Systems, ETH Zurich, Zurich/Switzerland
[3]Faculty of Architecture, University of Manitoba, Winnipeg/Canada
[4]School of Architecture and Landscape Architecture, UBC, Vancouver/Canada

Abstract: Urban trees can face heat stress from surrounding built materials. This paper proposes a raytracing framework that integrates LiDAR and tree species trait data with a biophysical model to simulate hourly leaf temperatures and species-specific physiological responses. Simulating 25 scenarios with 147 trees reveals that the landscape vegetation ratio is more effective at reducing heat stress than façade vegetation. High landscape coverage decreased risk by 5.2%, whereas high façade vegetation could increase risk by up to 12.8%. This open source workflow enables landscape architects to make data-driven material decisions to enhance urban forest health.

Keywords: Tree health, heat stress, microclimate modelling, raytracing, urban forest

1 Introduction

As cities experience longer and hotter summers, landscape architects are increasingly called upon to design outdoor spaces with cooling benefits (AKBARI et al. 2001, BARTESAGHI KOC et al. 2018, WU et al. 2025). Tree planting and material selections are two effective design strategies to mitigate overheating in urban microclimates (HAYES et al. 2022). At the same time, high-albedo (i. e., highly reflective) materials such as metal roofing and single-ply membranes are common architectural strategies for lowering air temperatures (FALASCA et al. 2019, SCHNEIDER et al. 2023). While the combination of materials with high-albedo and denser tree canopies could potentially improve urban temperature conditions (ELGENDY et al. 2025), high-albedo materials can induce acute heat stress in nearby trees (ERELL et al. 2014), even in cool temperate cities (KONARSKA et al. 2023, RISSANEN et al. 2024).

Tools such as ENVI-met (BRUSE & FLEER 1998) allow researchers and designers to investigate air temperature and outdoor thermal comfort under different planting scenarios, accounting for interactions among climate, trees, buildings, pavement, and other vegetated surfaces. Yet these tools come at a high cost, making them less accessible to researchers and landscape architects. While ENVI-met provides databases for materials and vegetation processes, users frequently rely on generic inputs and simplified canopy models, which can limit the authenticity of simulations in reflecting tree structures and site-specific surface material conditions. This gap limits landscape architects' capacity to make data-driven decisions about strategies that influence not only human thermal comfort but also the health of urban trees.

This paper proposes a modelling procedure capable of producing spatially detailed, temporally frequent data on the potential heat stress of trees. Specifically, we use datasets familiar to landscape architects (e. g., point cloud and tree species trait data) alongside high-fidelity, physics-based simulations developed by building and urban scientists (e. g., raytracing).

Journal of Digital Landscape Architecture, 11-2026, pp. 493-501. © Wichmann Verlag, VDE VERLAG GMBH · Berlin · Offenbach. ISBN 978-3-87907-770-0, ISSN 2367-4253, e-ISSN 2511-624X, doi:10.14627/537770048.

2 Assessing Heat Stress of Urban Trees

This method deploys a coupled surface-leaf-soil biophysical model to evaluate urban tree heat stress under alternative surface material scenarios (Fig. 1). The site model, described in Sec. 2.1, simulates hourly leaf temperature by integrating: high fidelity raytracing through Radiance (LARSON & SHAKESPEARE 1998) (Sec. 2.2), landscape and façade surface energy balance (Sec. 2.3), and the resulting biophysical stress on trees in the site (Sec. 2.4). The workflow supports scenario comparison for both landscape and façade materials by propagating the same material properties from raytracing to the biophysical calculations.

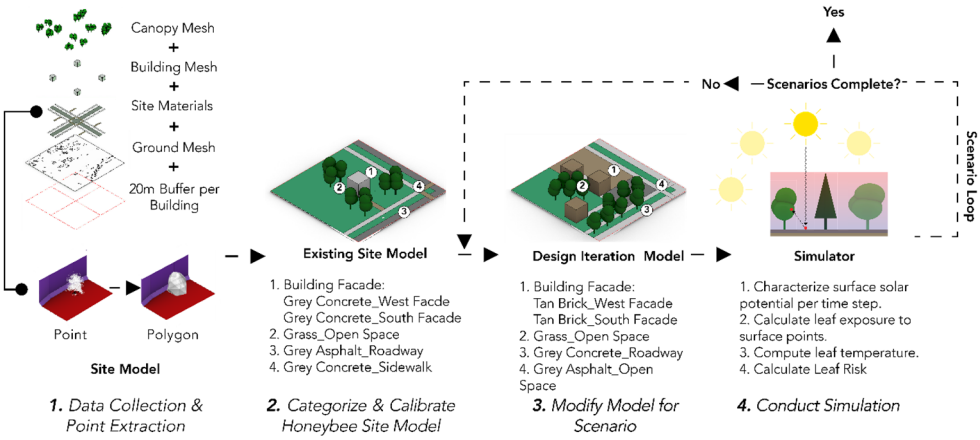

Fig. 1: The workflow for the project begins from data collection, digital elements assembly to the simulation loop phase

2.1 Digital Sandbox Assembly

The study site is in Winnipeg, Canada (49.90°N, 97.23°W). A digital base model was assembled to represent building volumes, façade and ground materials, with 147 on-site trees representing 33 species common to the region. Opaque surfaces were parameterized with material properties required for radiative and thermal calculations, emphasizing shortwave albedo (α) and longwave emissivity (ε), and materials were grouped as landscape (horizontal ground) or façade (vertical wall surfaces). Field survey is combined with building models and aerial laser surveys (CITY OF WINNIPEG 2021) of site vegetation to construct this base model (Fig. 2).

This base model represents the site's physical conditions (e. g., road networks, buildings, trees and other vegetated surfaces). It is semantically descriptive of surface materials (e. g., short grass, asphalt, grey cement pavers). This model was then translated into a Radiance project with a 1x1 meter point grid above the ground surface for physically accurate raytracing and the evaluation of surface solar gains within the model. The simulation produces a gridded time-series of direct beam irradiance and diffuse irradiance (i. e., surface solar potentials, or SP). These were then used to characterize the thermal environment around each tree.

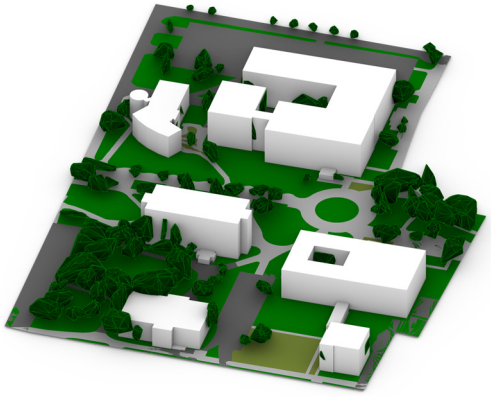

Fig. 2:
A 3D isometric representation (from the Southeast view) of the digital site simulation model

2.2 Raytracing Model Setup

To assess leaf risk (i. e., heat stress on foliage), 25 scenarios with fixed geometry and updated optical and thermal properties were defined and simulated based on combinations of landscape vegetation ratio (LVR, the percentage of horizontal space covered by vegetation) and façade vegetation ratio (FVR, the percentage of façade space covered by vegetation). For each scenario, the Radiance outputs were coupled to a simple surface energy balance to estimate surface and air temperatures and mean radiant temperature (MRT, including reflected shortwave from bright pavements). For each tree, a leaf-energy balance (with species Leaf Area Index and leaf traits) yields leaf temperature and transpiration; soil moisture is estimated from surface permeability and irrigation assumptions.

2.2.1 Tree – "Sensor" Mapping

A total of 4,325 sample points were generated in the model and used as the simulation "sensors" between 3D radiative transfer and tree-scale biophysics. Each tree was assigned the nearest grid in a 3D Euclidean space. Hourly irradiance components simulated at the sensor were then attributed to the tree and used to drive the subsequent surface and leaf energy balance calculations. This nearest-sensor coupling preserves spatial heterogeneity from buildings and surface materials while remaining computationally tractable across many trees and scenarios.

Species-specific physiological parameters were compiled from published literature and the TRY Plant Trait Database (KATTGE et al. 2020) and applied consistently across scenarios. Key parameters included leaf absorptivity (α_{leaf}), leaf emissivity ($\varepsilon_{\text{leaf}}$), maximum stomatal conductance ($g_{s,max}$) and stress response thresholds. Parameters governing radiation interception, specifically the fraction of downwelling radiation intercepted from above and below, were assigned based on LiDAR-derived tree crown architecture. Sky view factor (SVF) was computed individually for each tree using an average of two vectors: horizontal and south facing but tilted 45˚ upward). SVF was used to characterize the local radiative environment. SVF represents the fraction of the sky hemisphere visible from a point and influences both longwave radiation exchange with the atmosphere and MRT.

2.2.2 Radiative Transfer and Irradiance Components

Hourly irradiance fields were simulated in Radiance 5.2 (LBNL-ETA 2025) using a two-phase, direct-diffuse workflow to resolve the radiative environment at each sensor point. Here, (K) denotes shortwave (solar) irradiance (Wm^{-2}). Upwelling shortwave at a sensor was approximated post-raytracing using local material albedo: $K_{\uparrow(i,t)} = \alpha_i \, K_{\downarrow(i,t)}$. Longwave radiation was calculated from atmospheric conditions and surface temperatures rather than explicit raytracing. Downwelling longwave from the sky ($L_{\downarrow(i,t)}$) was computed from air temperature and relative humidity using standard atmospheric emissivity relationships. Upwelling longwave from surfaces ($L_{\uparrow(i,t)}$) was calculated as $L_{\uparrow} = \varepsilon \, \sigma \, T_{\text{surf}}^4$, where surface temperature was determined from the ground energy balance (Section 2.4). All scenarios used identical geometry, sensor points, and Radiance settings, so differences in radiation forcing reflect only changes in material properties (α), (ε). These shortwave and longwave components were then used to compute net radiation in the ground and leaf energy balances.

2.3 Material Scenario Construction

Material scenarios were constructed to isolate the influence of urban surface properties on tree radiative forcing and physiological stress. A factorial design was employed with five levels each for the landscape naturalness ratio ($r_L \in \{0,0.25,0.5,0.75,1.0\}$) and façade naturalness ratio ($r_F \in \{0,0.25,0.5,0.75,1.0\}$), yielding 25 scenarios (Fig. 3). The naturalness ratio controls the fraction of surfaces assigned vegetation-like materials (high emissivity, moderate albedo) versus mineral/synthetic materials (lower albedo, representing concrete, asphalt, or brick).

Surface materials were assigned to landscape and façade elements via grid identifiers carried through the Radiance pipeline, enabling consistent mapping between simulated irradiance outputs and the underlying surfaces. Alternative scenarios were generated by swapping material assignments for selected landscape and/or façade elements while holding all other inputs constant (geometry, tree locations, sensor grid, and weather). Each scenario was then re-simulated in Radiance using the same direct-diffuse workflow to produce comparable hourly irradiance components at each sensor.

Scenario effects enter the energy balances primarily through shortwave absorption and longwave exchange. For example, the net shortwave at the surface can be expressed as:

$$K_{\text{net}}(t) = (1 - \alpha) \, K_{\downarrow}(t) - K_{\uparrow}(t)$$

Changing (α) modifies both local absorption and (via $(K_{\uparrow})$) the reflected field experienced by nearby trees. Scenario outputs were stored as sensor-grid time series and mapped to trees for biophysical evaluation.

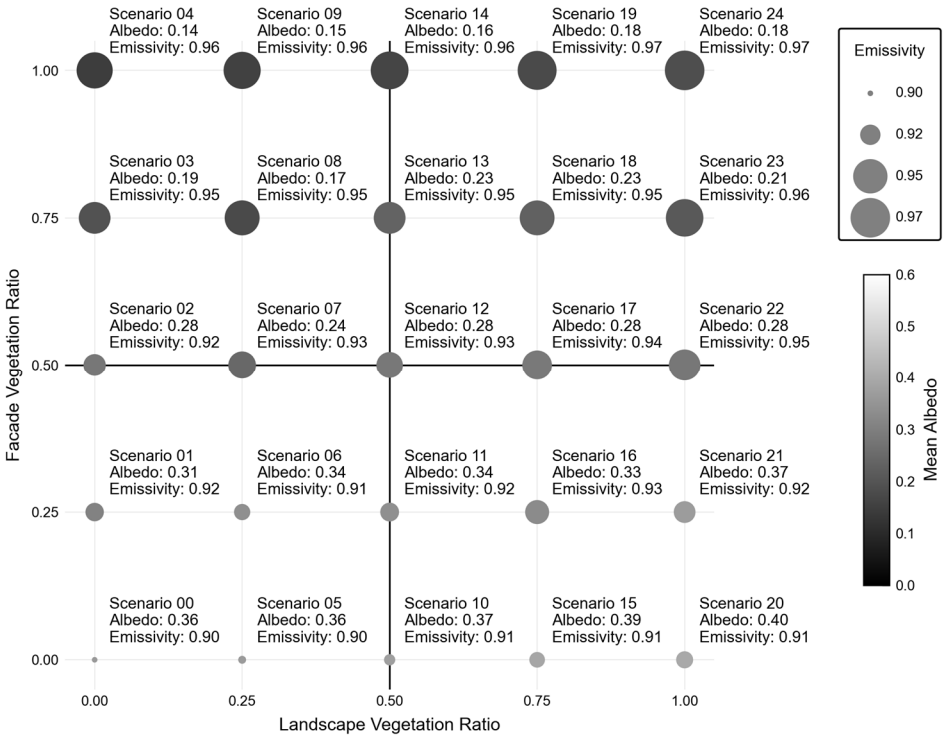

Fig. 3: The concept between the scenario development. Ratios refer to the percentage of total surfaces that are considered natural or not (i. e., concrete to grass).

2.4 Biophysical Stress

Tree stress was evaluated for the warmest week of the year (168 h), identified using a 7-day running mean of dry-bulb air temperature. For each tree and scenario, hourly ground temperature (T_g) was estimated using a one-layer surface energy balance accounting for thermal mass, absorbed shortwave (modulated by albedo), longwave exchange (modulated by emissivity), and sensible and latent heat fluxes. Material-specific heat capacity and evaporation factors (0 for impervious, 0.3-0.8 for pervious/vegetated surfaces) were assigned based on surface type. Leaf temperature (T_{leaf}) was then computed using the steady-state Canopy Energy Balance (CEB) model of Li et al. (2023), which takes scenario-specific shortwave irradiance and ground temperature as inputs. Material albedo affects leaf temperature through reflected shortwave, while emissivity affects it through ground cooling and upwelling longwave radiation.

We define stress (i. e., tree risk index) as the number of hours a leaf is above 30˚C. In this study, we use 30˚C heat stress as an efficiency risk (i. e., when leaf temperature is outside the optimal range) rather than a survival risk (DIAO et al. 2024). This model can also be parametrized to a higher temperature threshold (e. g., 42˚C) to avoid overly conservative simulations or to accommodate warmer climate conditions than those in Winnipeg. Scenario performance (i. e., biophysical stress of trees) was evaluated as stress reduction relative to the centre scenario (50%, 50%) in scenario 12 (Fig. 3).

3 Results and Discussion

3.1 Site Condition and Leaf Temperature Baseline

The site experienced a consistent daily pattern of ambient air temperature variation, except on July 1, 2025, when the temperature dropped to approximately 10°C. The median leaf temperature fluctuates in tandem with air temperature. SVF ranges from 0.10 to 0.19 across the site, reflecting the heterogeneous built environment surrounding each tree. Overall, the air temperature is marginally above the median leaf temperature during the day and below it at night. These results indicate that our simulated leaf temperature is responding well to the external climate variables.

3.2 Comparative Analysis of 25 Scenarios

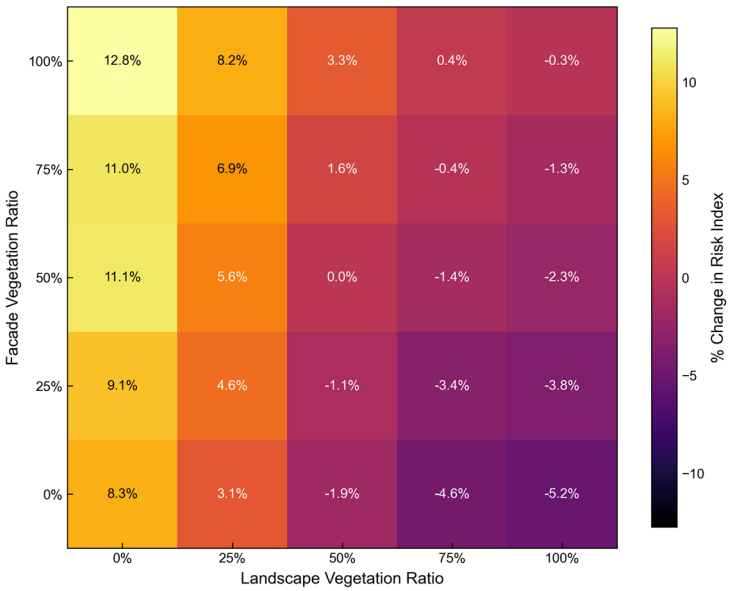

Fig. 4: Relative change in leaf risk in 25 simulated scenarios. The percent change was computed based on a 50/50 vegetation ratio (i. e., no change in risk index) in both the landscape and façade spaces.

Expectedly, as the LVR increases, tree risk decreases. This trend is consistent across façade FVRs (Fig. 4). We observe the greatest risk reduction when LVR is at its peak and when façade surfaces have minimal vegetation cover. However, for the same LVR, an increase in FVR (i. e., more vegetation cover on a given façade) will increase tree risk. In fact, the greatest increase in the risk index (+12.8%) occurs when FVR is 100%, and LVR is 0%.

This result is likely due to higher levels of landscape albedo (i. e., concrete is more reflective than vegetation) when ground vegetation cover is low. It is worth noting that the current implementation did not account for the emissivity of façade materials on nearby trees. It ac-

counted only for albedo during raytracing. Therefore, further work is needed to extend the leaf temperature model to account for multiple sources of exposure in longwave radiant transfer. There is discussion in the literature (SUSCA et al. 2022) on the impact of façade vegetation on mitigating heat in urban microclimates, and we identify the impact of emissivity as a current gap in this research.

3.3 Sensitivity Analysis

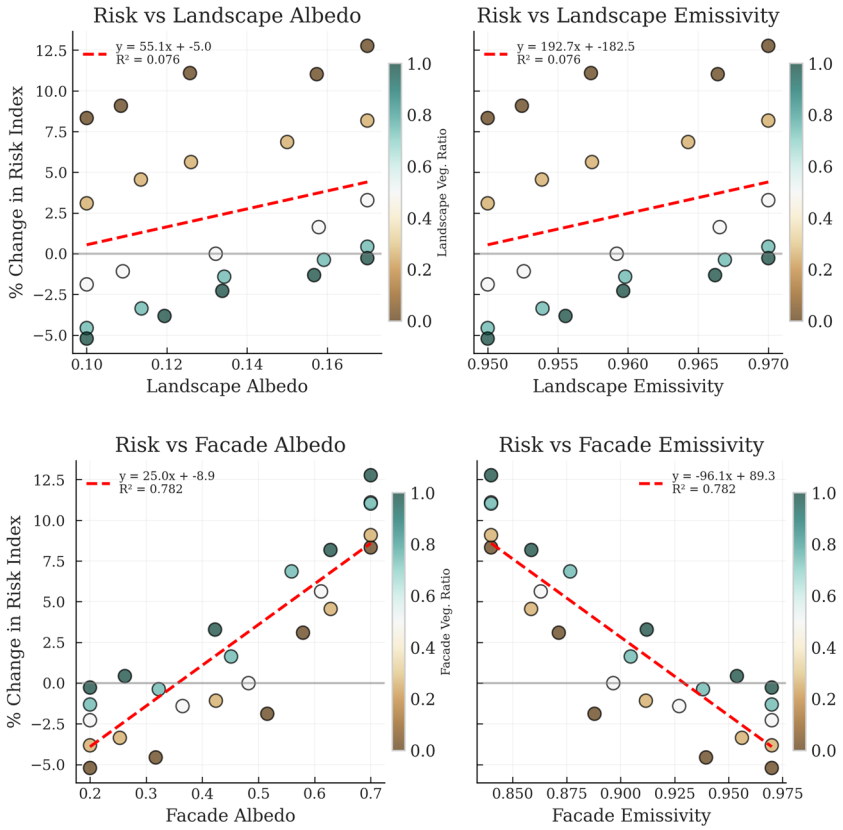

Fig. 5: Sensitivity analysis of the albedo and emissivity of the surfaces to the risk index

A sensitivity analysis further reveals how heat risk responds to different levels of material albedo and emissivity (Fig. 5). While facade emissivity is included, the relationship is superficial, as the model currently does not physically link the emissivity of the facade materials to leaf temperature. It is apparent that increases in albedo and emissivity lead to higher heat stress. With regards to the landscape material shift, a general linear trend can be observed across the landscape vegetation ratio spectrum (0 to 1, in Fig. 5). While the overall regression is weak, when fitted, a similar slope independently arises for each group. This is important to note, as the model accounts for ground temperature differently across material types, suggesting that it is not a more significant influence than emissivity or albedo alone. Future research is needed to follow up on this observation.

4 Conclusion and Outlook

This study integrates LiDAR-derived tree models, species trait data, and raytracing to simulate how material selections and planting patterns influence tree health. Crucially, the LVR emerged as the most effective strategy for mitigating heat stress, with the best-performing scenario reducing the tree risk index by 5.2% relative to the reference condition. This highlights a design paradox: increasing the FVR, intended to provide cooling, can inadvertently increase tree risk by up to 12.8% in certain configurations, due to the façade's higher albedo relative to conventional materials. This paper introduces an open-source "digital sandbox" that allows practitioners to test and measure the effects of materials and planting prior to construction, in contrast to commercial tools like ENVI-Met. Yet the unexpected increase in tree efficiency risk associated with façade vegetation warrants further research into façade emissivity and drought stress. Future work should make this model more accessible particularly to practitioners and expand the species-specific physiological parameters and validate the model across diverse climatic regions beyond Winnipeg.

Acknowledgement

We would like to thank the Landscape Architecture Canada Foundation (LACF #207 2026) and the Faculty of Architecture at the University of Manitoba for funding this research. The authors are also grateful for the valuable comments and edits from the reviewers and editors.

References

AKBARI, H., POMERANTZ, M. & TAHA, H. (2001), Cool surfaces and shade trees to reduce energy use and improve air quality in urban areas. Solar Energy, 70 (3), 295-310. https://doi.org/10.1016/S0038-092X (00)00089-X.

BARTESAGHI KOC, C., OSMOND, P. & PETERS, A. (2018), Evaluating the cooling effects of green infrastructure: A systematic review of methods, indicators and data sources. Solar Energy, 166 (March), 486-508. https://doi.org/10.1016/j.solener.2018.03.008.

BRUSE, M. & FLEER, H. (1998), Simulating surface-plant-air interactions inside urban environments with a three-dimensional numerical model. Environmental Modelling & Software, 13 (3-4), 373-384. https://doi.org/10.1016/S1364-8152 (98)00042-5.

CITY OF WINNIPEG (2021), Water and Waste LiDAR. https://data.winnipeg.ca/Water-and-Waste/Water-and-Waste-LiDAR/g634-qskh/about_data.

DIAO, H., CERNUSAK, L. A., SAURER, M., GESSLER, A., SIEGWOLF, R. T. W. & LEHMANN, M. M. (2024), Uncoupling of stomatal conductance and photosynthesis at high temperatures: mechanistic insights from online stable isotope techniques. New Phytologist. https://doi.org/10.1111/nph.19558.

ELGENDY, D., TOLBA, O. & KAMEL, T. (2025), The impact of increasing urban surface albedo on outdoor air and surface temperatures during summer in newly developed areas. Scientific Reports. https://doi.org/10.1038/s41598-025-08574-2.

ERELL, E., PEARLMUTTER, D., BONEH, D. & KUTIEL, P. B. (2014), Effect of high-albedo materials on pedestrian heat stress in urban street canyons. Urban Climate, 10 (P2), 367-386. https://doi.org/10.1016/j.uclim.2013.10.005.

FALASCA, S., CIANCIO, V., SALATA, F., GOLASI, I., ROSSO, F. & CURCI, G. (2019), High albedo materials to counteract heat waves in cities: An assessment of meteorology, buildings energy needs and pedestrian thermal comfort. Building and Environment, 163, 106242. https://doi.org/10.1016/j.buildenv.2019.106242.

HAYES, A. T., JANDAGHIAN, Z., LACASSE, M. A., GAUR, A., LU, H., LAOUADI, A., GE, H. & WANG, L. (2022), Nature-Based Solutions (NBSs) to Mitigate Urban Heat Island (UHI) Effects in Canadian Cities. Buildings 2022, Vol. 12, Page 925, 12 (7), 925. https://doi.org/10.3390/BUILDINGS12070925.

KATTGE, J., BÖNISCH, G., DÍAZ, S., LAVOREL, S., PRENTICE, I. C., LEADLEY, P., TAUTENHAHN, S., WERNER, G. D. A., AAKALA, T., ABEDI, M., ACOSTA, A. T. R., ADAMIDIS, G. C., ADAMSON, K., AIBA, M., ALBERT, C. H., ALCÁNTARA, J. M., ALCÁZAR C, C., ALEIXO, I., ALI, H., WIRTH, C. (2020), TRY plant trait database – enhanced coverage and open access. Global Change Biology, 26 (1), 119-188. https://doi.org/10.1111/gcb.14904;ctype:string:journal.

KONARSKA, J., TARVAINEN, L., BÄCKLIN, O., RÄNTFORS, M. & UDDLING, J. (2023), Surface paving more important than species in determining the physiology, growth and cooling effects of urban trees. Landscape and Urban Planning, 240, 104872. https://doi.org/10.1016/j.landurbplan.2023.104872.

LARSON, G. W. & SHAKESPEARE, R. (1998), Rendering with Radiance: the art and science of lighting visualization. Morgan Kaufmann Publishers. https://books.google.com/books/about/rendering_with_radiance.html?id=dupsaaaamaaj.

LBNL-ETA (2025), LBNL-ETA/pyradiance: Python wrapper for the validated RADIANCE ray-tracing engine. https://github.com/LBNL-ETA/pyradiance.

LI, R., ZENG, F., ZHAO, Y., WU, Y., NIU, J., WANG, L., GAO, N., ZHOU, H., SHI, X. & HUANG, Z. (2023), Analyzing the impact of various factors on leaf surface temperature based on a new tree-scale canopy energy balance model. Sustainable Cities and Society, 99. https://doi.org/10.1016/j.scs.2023.104994.

RISSANEN, K., LAPA, G., HOULE, D., KNEESHAW, D. & PAQUETTE, A. (2024), Large variation in the radial patterns of sap flow among urban trees. Agricultural and Forest Meteorology, 345, 109848. https://doi.org/10.1016/J.AGRFORMET.2023.109848.

SCHNEIDER, F. A., ORTIZ, J. C., VANOS, J. K., SAILOR, D. J. & MIDDEL, A. (2023), Evidence-based guidance on reflective pavement for urban heat mitigation in Arizona. Nature Communications, 14 (1), 1-12. https://doi.org/10.1038/S41467-023-36972-5.

SUSCA, T., ZANGHIRELLA, F., COLASUONNO, L. & DEL FATTO, V. (2022), Effect of green wall installation on urban heat island and building energy use: A climate-informed systematic literature review. Renewable and Sustainable Energy Reviews, 159, 112100. https://doi.org/10.1016/J.RSER.2022.112100.

WU, Y., MASHHOODI, B. & PATUANO, A. (2025), Effective street tree and grass designs to cool European neighbourhoods. Urban Climate, 61, 102376. https://doi.org/10.1016/J.UCLIM.2025.102376.